DISCRETE AND CONTINUOUS
DYNAMICAL SYSTEMS
Volume **41**, Number **4**, April **2021**

doi:10.3934/dcds.2020343

pp. **1875–1895**

REVERSIBLE PERTURBATIONS OF CONSERVATIVE HÉNON-LIKE MAPS

Marina Gonchenko

Universitat Politècnica de Catalunya, Barcelona, Spain

Sergey Gonchenko

Mathematical Center "Mathematics of Future Technologies"
Lobachevsky State University of Nizhny Novgorod, Nizhny Novgorod, Russia
and
Laboratory of Dynamical Systems and Applications
National Research University Higher School of Economics, Nizhny Novgorod, Russia

Klim Safonov

Laboratory of Dynamical Systems and Applications
National Research University Higher School of Economics, Nizhny Novgorod, Russia

(Communicated by Jiangong You)

Abstract. For area-preserving Hénon-like maps and their compositions, we consider smooth perturbations that keep the reversibility of the initial maps but destroy their conservativity. For constructing such perturbations, we use two methods, a new method based on reversible properties of maps written in the so-called cross-form, and the classical Quispel-Roberts method based on a variation of involutions of the initial map. We study symmetry breaking bifurcations of symmetric periodic orbits in reversible families containing quadratic conservative orientable and nonorientable Hénon maps as well as a product of two Hénon maps whose Jacobians are mutually inverse.

1. **Introduction.** Among dynamical systems of various classes, the so-called *reversible systems* are of special interest that can be explained by two main reasons. First, such systems often appear in applications [20, 26], and second, they require the development of very specific mathematical methods for their study [3, 27, 28]. In this paper we study two-dimensional reversible maps.

Recall that a C^r-map (diffeomorphism) f is said to be *reversible* if it is conjugate to its inverse f^{-1} by an involution $\mathcal{G}$, i.e. the following condition holds $f = \mathcal{G} \circ f^{-1} \circ \mathcal{G}$, where $\mathcal{G}^2 = \mathrm{id}$ and the diffeomorphism $\mathcal{G}$ is also at least C^r-smooth.

Recently, the study of dynamics of reversible systems has got a new motivation due to the discovery of the new, third, form of dynamical chaos, the so-called *mixed dynamics* [10, 12], which is characterized by the principal inseparability of dissipative elements of dynamics (attractors and repellers) from conservative ones. The above property makes mixed dynamics fundamentally different from the two other classical forms of chaos, conservative and dissipative.

2020 *Mathematics Subject Classification.* Primary: 37G25, 37G40; Secondary: 37C70.

Key words and phrases. area-preserving Hénon-like map, symmetry breaking bifurcation, reversible diffeomorphism, mixed dynamics, pitchfork bifurcation.

Conservative dynamics is demonstrated by Hamiltonian systems or, more generally, systems preserving the phase volume, and, from the point of view of topological dynamics, is characterized by the fact that the entire phase space of the corresponding system is chain-transitive [12].

Dissipative dynamics has a completely different nature: it is associated with the existence of "holes" (absorbing and repelling domains) in the phase space M. Recall that an open domain D is said to be absorbing (repelling) if the image of its closure under the action of a map T (a map T^{-1}) lies strictly inside it. By definition, a dissipative attractor, closed stable invariant set, resides in some absorbing domain D_a, analogously, a (dissipative) repeller resides in some repelling domain D_r, and these domains do not intersect ($D_a \cap D_r = \emptyset$).

As for mixed dynamics, unlike the conservative case, the phase space is not chain-transitive, since infinitely many dissipative attractors and repellers can exist here, and their closures intersect along closed invariant sets, the so-called reversible cores [12], having neutral (conservative-like) type of stability. The latter means that the reversible core itself attracts nothing and repels nothing – for any nearby point, the forward orbit tends to the nearest attractor and the backward orbit tends to the nearest repeller.[1] In other words, here, unlike the dissipative case, it is impossible to construct a set of disjoint absorbing and repelling domains. The explanation of this phenomenon from the topological point of view was given in [12] based on the concept of attractor going back to D. Ruelle [30].

Certainly, mixed dynamics is not the peculiarity of reversible systems only. As follows from [15], it can arise in general systems, which somewhere contract phase volumes, and somewhere expand them, and the corresponding regions of the phase space are not dynamically separated from each other - e.g. there are heteroclinic connections between saddle periodic orbits with the Jacobians greater than 1 and less than 1. For reversible non-conservative systems, both of these properties are quite natural – their attractors and repellers are always symmetric to each other, they can intersect along a reversible core, which is always self-symmetric (under the involution) and contains the explicit conservative elements, such as symmetric elliptic periodic orbits [12, 16]. In the case of general systems, the conservative nature of reversible cores is still completely unknown, and, in this sense, reversible systems are special and, therefore, interesting.

One of the main fundamental properties of systems with mixed dynamics, which can also be considered as a criterion and even as its definition, is the existence of the so-called *absolute Newhouse regions* [15, 34, 35]. Recall that Newhouse regions are open regions in the space of dynamical systems (or in the parameter space) in which systems with homoclinic tangencies are dense (or values of parameters corresponding to systems with homoclinic tangencies are dense) [14, 23, 25, 29]. It was shown by Newhouse himself [24] that, in the dissipative case, there may exist Newhouse regions in which systems with infinitely many stable and saddle periodic orbits are dense and, moreover, generic, i.e., they form subsets of the second Baire category. The absolute Newhouse regions are characterized by the following property: systems with infinitely many periodic orbits of all possible types (sinks, sources, and saddles) are generic in such regions, and these orbits are inseparable from each other, i.e., the closures of the sets of orbits of different types have nonempty intersections.

[1]Note that the reversible core can be vast and occupy a large part of the phase space and, thus, mixed dynamics becomes an observable phenomenon in applications, see e.g. [6, 7, 8, 13, 18, 19].

The absolute Newhouse regions exist for two-dimensional reversible maps as well [4, 17, 21]. Moreover, the dynamics of systems from reversible absolute Newhouse regions is much richer than for those in the general case. In particular, as shown in [21], diffeomorphisms with infinitely many coexisting periodic sinks, sources, and symmetric elliptic periodic orbits are generic in reversible absolute Newhouse regions.

A periodic orbit of a reversible map f is called *symmetric* if it is invariant with respect to the involution $\mathcal{G}$, i.e., if its points are posed $\mathcal{G}$-symmetrically around the set $\mathrm{Fix}(\mathcal{G}) = \{x : \mathcal{G}(x) = x\}$ of fixed points of the involution, thus, if Q is such an orbit, then $Q = \mathcal{G}(Q)$. Note that a symmetric orbit should have intersection points either with $\mathrm{Fix}(\mathcal{G})$ or with $\mathrm{Fix}(f \circ \mathcal{G})$, where $f \circ \mathcal{G}$ is always the second involution for f. In the two-dimensional case, a symmetric periodic orbit of an orientable reversible map f has multipliers λ and λ^{-1}. In the general case $\lambda \neq \lambda^{-1}$, symmetric periodic points can be divided into two types: saddle points, if $\lambda \neq \pm 1$ is real, and elliptic points, if $\lambda_{1,2} = e^{\pm i\varphi}$ and $0 < \varphi < \pi$. The saddle points are structurally stable. As for elliptic points, although they are very similar to conservative elliptic points [32], they can differ greatly from the latter, as shown by the following results [12, 16]:

- *all symmetric elliptic periodic orbits of a C^r-generic ($r = 1, ..., \infty$) two-dimensional reversible map are the limits of periodic sinks and sources.*[2]
- *all symmetric elliptic periodic orbits of a C^r-generic ($r = 1, ..., \infty$) two-dimensional reversible map are reversible cores;*
- *the generic elliptic periodic point of a reversible map is totally stable (or stable under permanently acting perturbations), while in the case of area-preserving maps any such orbit is unstable (although it is Lyapunov orbitally stable).*

Thus, the reversible mixed dynamics manifests itself locally wherever symmetric elliptic points exist. This important circumstance, of course, testifies to the fact that mixed dynamics should be viewed as one of the fundamental properties of reversible systems. Moreover, the above results show that symmetric (elliptic and other) orbits form a skeleton of global mixed dynamics, as they compose naturally that invariant set, reversible core, which simultaneously separates and connects the attractor and repeller.

The other important circumstance testifying to the universality of mixed dynamics in reversible systems is the so-called Reversible Mixed Dynamics (RMD) conjecture:

- *Near any reversible map with a symmetric homoclinic tangency or a symmetric nontransversal heteroclinic cycle, there are absolute reversible Newhouse regions.*

This RMD-conjecture was proposed in [4] and was almost immediately proved in [16] for Newhouse regions from the space of reversible systems in the C^r-topology with $2 \leq r \leq \infty$. In the analytical case, as well as in the case of parameter families, the RMD-conjecture was proved only for the so-called a priori non-conservative reversible diffeomorphisms [5, 17, 21], when a heteroclinic cycle contains non-conservative elements (for example, saddles with the Jacobians greater and less than 1, or pairs of nonsymmetric homoclinic tangencies of a symmetric

[2]The genericity is understood here in the sense that reversible maps with the indicated properties form a subset of the second Baire category in the space of C^r-smooth reversible maps having symmetric elliptic periodic orbits.

saddle point, as in [5]), as well as for reversible maps with symmetric heteroclinic cycles of conservative type [4].

Essentially, it remains to consider only two most interesting cases: *reversible maps with symmetric quadratic and cubic homoclinic tangencies*. However, these two cases are also the most difficult, since, in principle, the main problem of this topic is connected with the study of symmetry breaking bifurcations in first return maps constructing near orbits of symmetric homoclinic tangencies. In the main order, these maps coincide with the conservative Hénon-like maps: the conservative Hénon map $\bar{x} = y,\ \bar{y} = M - x - y^2$ (when the tangency is quadratic) and the reversible cubic Hénon maps $\bar{x} = y,\ \bar{y} = -x + My \pm y^3$ (appearing near symmetric cubic homoclinic tangencies of two different types [9]).

Both these maps are only certain truncated normal forms for the complete first return maps, and they demonstrate exclusively conservative dynamics. What can be said about the dynamics of these maps under perturbations that keep the reversibility, and how can dissipative elements appear here, such as periodic sinks, sources, or saddles with the Jacobians other than 1? This is still open problem which requires solving the following issues.

- How to construct perturbations of area-preserving Hénon-like maps which maintain their reversibility, but destroy the conservativity?
- What is the structure of symmetry breaking bifurcations under such perturbations?

In the current paper we deal with these questions. Accordingly, the paper is divided into two parts. In the first one, Sections 2 and 3, we consider two methods for the construction of reversible perturbations for conservative Hénon-like maps. The first method looks to be new: we call it "cross-form perturbations", see Section 2.1. We apply this method to the conservative Hénon-like maps of the form $\bar{x} = y, \bar{y} = -x + F(y)$, see Section 2.2, and for compositions of two Hénon-like maps, see Sections 2.3 and 2.4. The second method is the classical method proposed in the paper [28] by Quispel and Roberts. We apply this Quispel-Roberts method for the above Hénon-like maps in Section 3 and for the nonorientable conservative Hénon-like maps of the form $\bar{x} = -y, \bar{y} = -x + F(y)$ in Section 3.1.[3]

In the second part of the paper, Section 4, we study symmetry breaking bifurcations in one-parameter families of reversible non-conservative Hénon-like maps, using those perturbations that have been constructed in the first part of the paper. We show that the simplest bifurcations of this type are reversible pitchfork bifurcations of periodic orbits. We consider such families in the cases of the product of two (quadratic) Hénon maps (Section 4.1), the nonorientable conservative Hénon map (Section 4.2) and the orientable conservative Hénon map (Sections 4.3 and 4.4). In the first two cases we show that even symmetric fixed points can undergo pitchfork bifurcations and recover their structure. It is interesting that, in the case of orientable conservative Hénon map, this bifurcation occurs starting only with an orbit of period 6 (no such bifurcation takes place for orbits of less period), that is very surprising.

[3]Note that, formally, the cross-form perturbations method and Quispel-Roberts method give different results, at first sight. Of course, the Quispel-Roberts method is more general, since this method can be applied to any reversible maps, however, it is not very clear how certain perturbations can be obtained by means of it, in particular, those that the cross-form method gives.

2. **On construction of reversible perturbations for Hénon-like maps and their compositions.** The conservative Hénon-like maps are the two-dimensional planar diffeomorphisms that can be represented in the form

$$H: \ \bar{x} = y, \quad \bar{y} = -x + F(y), \tag{1}$$

where $F(y)$ is some nonlinear function (e.g. a polynomial). Map (1) is area-preserving, with the Jacobian equal to 1, and reversible with respect to the linear involution $h: (x, y) \to (y, x)$. Indeed, H^{-1} takes the form $x = \bar{y}, y = -\bar{x} + F(\bar{y})$; the relation $h \circ H^{-1} \circ h$ means, due to the simplicity of h, that we need to make interchanges $x \leftrightarrow y, \bar{x} \leftrightarrow \bar{y}$ in the formula for H^{-1}, after which we get (1).

In this section we consider the cross-form method for construction of such sufficiently smooth (analytic) perturbations of Hénon-like maps (1) and their compositions that destroy the conservativity of these maps but keep their reversibility with respect to the involution h.

2.1. **Cross-form perturbations.** The first method to obtain reversible perturbations is based on the following cross-form map

$$g: (x, y) \to (\bar{x}, \bar{y}) \ : \quad \bar{x} = G(x, \bar{y}), \quad y = G(\bar{y}, x). \tag{2}$$

Note that map (2) is reversible with respect to the involution $h: (x, y) \to (y, x)$. The proof is immediate: map g^{-1} takes the form $x = G(\bar{x}, y), \quad \bar{y} = G(y, \bar{x})$, and the composition $h \circ g^{-1} \circ h$ means that we need to make interchanges $x \leftrightarrow y$ and $\bar{x} \leftrightarrow \bar{y}$ in g^{-1}, which leads to (2).

We introduce certain notations for the derivatives of functions:

- $F'(\rho)$ denotes the first derivative of the function $F(y)$ at the point $y = \rho$;
- for a smooth function $s(x, y)$, we denote

$$u(x, y) = \frac{\partial s(x, y)}{\partial x}, \ \ v(x, y) = \frac{\partial s(x, y)}{\partial y}.$$

and

$$s_x(\xi, \eta) = u(\xi, \eta), \ s_y(\xi, \eta) = v(\xi, \eta).$$

Thus, the subscripts x and y means the differentiation with respect to the first and second variables, respectively.

Lemma 2.1. *The Jacobian of map (2) takes the form*

$$J \ = \ \frac{G_x(x, \bar{y})}{G_x(\bar{y}, x)} \tag{3}$$

Proof. It follows from (2) that

$$\frac{\partial \bar{x}}{\partial x} = G_x(x, \bar{y}) + G_y(x, \bar{y}) \frac{\partial \bar{y}}{\partial x}, \ \ \frac{\partial \bar{x}}{\partial y} = G_y(x, \bar{y}) \frac{\partial \bar{y}}{\partial y},$$

$$0 = G_x(\bar{y}, x) \frac{\partial \bar{y}}{\partial x} + G_y(\bar{y}, x), \ \ 1 = G_x(\bar{y}, x) \frac{\partial \bar{y}}{\partial y}$$

Then we get

$$\frac{\partial \bar{y}}{\partial y} = \frac{1}{G_x(\bar{y}, x)}, \ \frac{\partial \bar{y}}{\partial x} = -\frac{G_y(\bar{y}, x)}{G_x(\bar{y}, x)},$$

$$\frac{\partial \bar{x}}{\partial x} = G_x(x, \bar{y}) - \frac{G_y(x, \bar{y}) G_y(\bar{y}, x)}{G_x(\bar{y}, x)}, \ \frac{\partial \bar{x}}{\partial y} = \frac{G_y(x, \bar{y})}{G_x(\bar{y}, x)},$$

and, as a result, we deduce formula (3) for the Jacobian $J = \partial \bar{x}/\partial x \cdot \partial \bar{y}/\partial y \ - \partial \bar{x}/\partial y \cdot \partial \bar{y}/\partial x$. □

Therefore, once having a conservative map written in the implicit form (2), we can simply add a perturbation in such a way that the cross-form is preserved, and the perturbed system will be reversible.

2.2. **Cross-form perturbation of (1).** The idea to write a cross-form perturbation for map H, given in (1), comes from a possibility to present the second equation of (1) in the form $y = F^{-1}(x + \bar{y})$, where F^{-1} is a formal operator. Then map H is rewritten in cross-form (2) as follows

$$H:\ \bar{x} = F^{-1}(x + \bar{y}), \quad y = F^{-1}(\bar{y} + x).$$

Thus, perturbations of the form

$$\tilde{H}:\ \bar{x} = F^{-1}(x + \bar{y}) + \varepsilon(x, \bar{y}), \quad y = F^{-1}(\bar{y} + x) + \varepsilon(\bar{y}, x)$$

are formally reversible. For the corresponding map $\tilde{H}$ we obtain from the second equation that $F^{-1}(\bar{y} + x) = y - \varepsilon(\bar{y}, x)$ and, thus, $\bar{y} + x = F(y - \varepsilon(\bar{y}, x))$. Then map $\tilde{H}$ takes the following form

$$\tilde{H}:\ \bar{x} = y + \varepsilon(x, \bar{y}) - \varepsilon(\bar{y}, x), \quad \bar{y} = -x + F(y - \varepsilon(\bar{y}, x)). \tag{4}$$

By construction, map (4) should be reversible, however, the operator F^{-1} is only formal, therefore, the reversibility of $\tilde{H}$ should be verified directly. This is done in the following lemma.

Lemma 2.2. *The map $\tilde{H}$, defined in (4), is reversible with respect to the involution $h : (x, y) \to (y, x)$.*

Proof. To prove the reversibility of $\tilde{H}$, we have to show that $\tilde{H} = h \circ \tilde{H}^{-1} \circ h$. The inverse map $\tilde{H}^{-1}$ is obtained after swapping the bar and no-bar variables $\bar{x} \leftrightarrow x, \bar{y} \leftrightarrow y$, i.e.,

$$\tilde{H}^{-1}\ :\quad \bar{x} = -y + F(\bar{y} - \varepsilon(y, \bar{x})), \quad \bar{y} = x - \varepsilon(\bar{x}, y) + \varepsilon(y, \bar{x}). \tag{5}$$

After exchanging $x \leftrightarrow y$ and $\bar{x} \leftrightarrow \bar{y}$ in (5), due to the involution h, we get the expression for $h \circ \tilde{H}^{-1} \circ h$ which coincides with (4). □

Lemma 2.3. *The Jacobian of map (4) takes the following formula*

$$J = \frac{1 + F'(y - \varepsilon(\bar{y}, x))\varepsilon_x(x, \bar{y})}{1 + F'(y - \varepsilon(\bar{y}, x))\varepsilon_x(\bar{y}, x)}. \tag{6}$$

Proof. Differentiating the first equation of (4) with respect to x and y we get

$$\frac{\partial \bar{x}}{\partial x} = \varepsilon_x(x, \bar{y}) + \varepsilon_y(x, \bar{y})\frac{\partial \bar{y}}{\partial x} - \varepsilon_x(\bar{y}, x)\frac{\partial \bar{y}}{\partial x} - \varepsilon_y(\bar{y}, x),$$
$$\frac{\partial \bar{x}}{\partial y} = 1 + \varepsilon_y(x, \bar{y})\frac{\partial \bar{y}}{\partial y} - \varepsilon_x(\bar{y}, x)\frac{\partial \bar{y}}{\partial y}.$$

Therefore, we have

$$J = \frac{\partial \bar{x}}{\partial x}\frac{\partial \bar{y}}{\partial y} - \frac{\partial \bar{x}}{\partial y}\frac{\partial \bar{y}}{\partial x} = (\varepsilon_x(x, \bar{y}) - \varepsilon_y(\bar{y}, x))\frac{\partial \bar{y}}{\partial y} - \frac{\partial \bar{y}}{\partial x}. \tag{7}$$

We find the derivatives $\partial\bar{y}/\partial x$ and $\partial\bar{y}/\partial y$ from the second equation of (4) by its implicit differentiation

$$\frac{\partial \bar{y}}{\partial x} = \frac{-1 - F'(y - \varepsilon(\bar{y}, x))\varepsilon_y(\bar{y}, x)}{1 + F'(y - \varepsilon(\bar{y}, x))\varepsilon_x(\bar{y}, x)}, \quad \frac{\partial \bar{y}}{\partial y} = \frac{F'(y - \varepsilon(\bar{y}, x))}{1 + F'(y - \varepsilon(\bar{y}, x))\varepsilon_x(\bar{y}, x)}.$$

After substituting these into (7), we obtain (6). □

It is worth mentioning that if the perturbation $\varepsilon(x,y)$ in (4) is a symmetric function, i.e. $\varepsilon(x,y)=\varepsilon(y,x)$, the perturbed map (4) takes the simpler form

$$\tilde{H}:\ \bar{x}=y,\quad \bar{y}=-x+F(y-\varepsilon(x,\bar{y})), \tag{8}$$

and the same formula (6) holds for the Jacobian.

Note that the perturbed systems (4) and (8) contain perturbing terms inside a nonlinear function F, and, hence, it is hard to iterate the maps – one needs to solve the second equation for $\bar{y}$ and calculate $\bar{y}=f(x,y)$. In Sections 2.3 and 2.4 we show that using cross-form (2) it is possible to construct reversibility preserving perturbations of other kinds which allows to iterate the resulting maps directly. We also show in Section 3 that such explicit perturbations can be constructed by the Quispel-Roberts method.

2.3. **Perturbations of H^{-2}.** The cross-form reversible perturbations can be easily constructed for the map H^{-2} that is the square of the inverse map H^{-1} of the conservative Hénon-like map H. We obtain from (1) that map H^{-1} takes the form

$$H^{-1}:\quad \bar{x}=-y+F(x),\quad \bar{y}=x.$$

Then map $H^{-2}=H^{-1}\circ H^{-1}$ is written as

$$H^{-2}:\quad \bar{x}=-x+F(-y+F(x)),\quad \bar{y}=-y+F(x), \tag{9}$$

Lemma 2.4. *Map $\tilde{H}^{-2}$ of the form*

$$\tilde{H}^{-2}:\quad \bar{x}=-x+F(\bar{y})+\varepsilon(x,\bar{y}),\quad \bar{y}=-y+F(x)+\varepsilon(\bar{y},x) \tag{10}$$

is a reversible perturbation of H^{-2} with respect to the involution $h:(x,y)\to(y,x)$. The Jacobian of $\tilde{H}^{-2}$ is

$$J=\frac{1-\varepsilon_x(x,\bar{y})}{1-\varepsilon_x(\bar{y},x)}.$$

Proof. Map (9) can be presented as follows

$$H^{-2}:\quad \bar{x}=-x+F(\bar{y}),\quad y=-\bar{y}+F(x),$$

which is the cross-form (2) with $G(x,y)=-x+F(y)$. Then the perturbed map (10) preserves cross-form (2) with new $G(x,y)=-x+F(y)+\varepsilon(x,y)$. The desired formula for the Jacobian $J(\tilde{H}^{-2})$ is obtained now from (3). □

Form (10) of $\tilde{H}^{-2}$ allows to write the map explicitly for certain perturbations. For example, if $\varepsilon(x,y)$ is linear in x, i.e. $\varepsilon(x,y)=\alpha(y)+x\beta(y)$, then the map yields

$$\tilde{H}^{-2}:\quad \bar{x}=-x+F(\bar{y})+\alpha(\bar{y})+x\beta(\bar{y}),\quad \bar{y}=\frac{-y+F(x)+\alpha(x)}{1-\beta(x)}$$

and its Jacobian is

$$J=\frac{1-\beta(\bar{y})}{1-\beta(x)}.$$

Hence, the new map is a diffeomorphism in some ball $\{x\in\mathbb{R}:\|(x,y)\|\le R_\beta\}$, where $R_\beta\to\infty$ as $|\beta|\to 0$. Besides, for some special functions $\beta(x)$ (for instance, $\beta(x)=\mu\arctan(x)$ with sufficiently small μ), the map is an analytical diffeomorphism in the whole plane $\mathbb{R}^2$.

2.4. **Perturbations of compositions of two asymmetric Hénon-like maps.** The next approach is connected with constructing perturbations for the product of two asymmetric (non-conservative, in general) Hénon-like maps H_1 and H_2 of the form

$$H_1: \quad \bar{x} = y, \quad \bar{y} = bx + F(y) \quad \text{and} \quad H_2: \quad \bar{x} = y, \quad \bar{y} = \frac{1}{b}x - \frac{1}{b}F(y). \tag{11}$$

These maps have the Jacobians $-b$ and $-1/b$, respectively, and their nonlinearities are asymmetric, since their inverse maps are

$$H_1^{-1}: \quad \bar{x} = \frac{1}{b}y - \frac{1}{b}F(x), \quad \bar{y} = x \quad \text{and} \quad H_2^{-1}: \quad \bar{x} = by + F(x), \quad \bar{y} = x,$$

respectively. The composition $H_{12}^{-1} = H_1^{-1} \circ H_2^{-1}$ of these maps can be written as

$$H_{12}^{-1}: \quad \bar{x} = \frac{1}{b}x - \frac{1}{b}F\left(by + F(x)\right), \quad \bar{y} = by + F(x),$$

or as

$$H_{12}^{-1}: \quad \bar{x} = \frac{1}{b}x - \frac{1}{b}F\left(\bar{y}\right), \quad y = \frac{1}{b}\bar{y} - \frac{1}{b}F(x). \tag{12}$$

in cross-form (2) with $G(x,y) = b^{-1}(x - F(y))$. This implies the following result

Lemma 2.5. *The map*

$$\tilde{H}_{12}^{-1}: \quad \bar{x} = \frac{1}{b}x - \frac{1}{b}F(\bar{y}) + \varepsilon(x,\bar{y}), \quad y = \frac{1}{b}\bar{y} - \frac{1}{b}F(x) + \varepsilon(\bar{y},x) \tag{13}$$

is a reversible perturbation of $H_1^{-1} \circ H_2^{-1}$ that keeps the involution $h: (x,y) \to (y,x)$, and

$$J\left(\tilde{H}_{12}^{-1}\right) = \frac{1 + b\varepsilon_x(x,\bar{y})}{1 + b\varepsilon_x(\bar{y},x)}. \tag{14}$$

3. **Quispel-Roberts method for construction of reversible perturbations.** The basic elements of the theory of reversible systems were developed in the famous paper [28] by Quispel and Roberts. In particular, in this paper general methods for the construction of reversible perturbations of reversible maps were proposed. One of such methods is based on the following two facts:

1) Any reversible map can be represented as a composition of its two involutions.
2) If ζ is an involution, then $\tilde{\zeta} = T^{-1} \circ \zeta \circ T$ is also involution, if the map T is a diffeomorphism.

Indeed, for item 1), if ζ is an involution of a map f, we have $f = \zeta \circ f^{-1} \circ \zeta = \zeta \circ \left(f^{-1} \circ \zeta\right)$ and the map $f^{-1} \circ \zeta$ is also involution, since

$$\left(f^{-1} \circ \zeta\right)^2 = f^{-1} \circ \zeta \circ f^{-1} \circ \zeta = f^{-1} \circ \left(\zeta \circ f^{-1} \circ \zeta\right) = f^{-1} \circ f = \text{ id}.$$

For item 2), we obtain

$$\tilde{\zeta}^2 = T^{-1} \circ \zeta \circ \left(T \circ T^{-1}\right) \circ \zeta \circ T = T^{-1} \circ (\zeta \circ \zeta) \circ T = T^{-1} \circ T = \text{ id}.$$

The conservative Hénon-like map H given by (1) can be also presented as the product $H = h_1 \circ h_2$ of two involutions:

$$h_1 = h: \begin{cases} \bar{x} = y, \\ \bar{y} = x \end{cases} \quad \text{and} \quad h_2: \begin{cases} \bar{x} = -x + F(y), \\ \bar{y} = y \end{cases} \tag{15}$$

Thus, we can construct reversible perturbations of H by means of changing their involutions. For our goals, we keep the involution $h_1 = h$ and take the new involution $\tilde{h}_2$ as a perturbation $\tilde{h}_2 = T^{-1} \circ h_2 \circ T$ of involution h_2 by means of a map

T that is close to the identity map $\bar{x} = x, \bar{y} = y$. The following lemma summarizes results of the corresponding calculations.

Lemma 3.1. *The map*

$$\hat{H} : \bar{x} = y + \varepsilon_2(x,y) - \varepsilon_2(\bar{y},\bar{x}),\ \bar{y} = -x + F\left(y + \varepsilon_2(x,y)\right) - \varepsilon_1(x,y) - \varepsilon_1(\bar{y},\bar{x}) \quad (16)$$

is a reversible perturbation of the conservative Hénon-like map H, given in (1), that is constructed in the form $\hat{H} = h_1 \circ \tilde{h}_2$, where $\tilde{h}_2 = T^{-1} \circ h_2 \circ T$ and the map $T:\ \bar{x} = x + \varepsilon_1(x,y), \bar{y} = y + \varepsilon_2(x,y)$ is assumed to be a near identity map.

Proof. We find first the new involution $\tilde{h}_2 = T^{-1} \circ h_2 \circ T$. By (15), the composition $h_2 \circ T : (x,y) \to (x',y')$ can be written as

$$h_2 \circ T : \begin{cases} x' = -x - \varepsilon_1(x,y) + F(y + \varepsilon_2(x,y)), \\ y' = y + \varepsilon_2(x,y). \end{cases}$$

We can write the map $T^{-1} : (x',y') \to (\bar{x},\bar{y})$ as follows $\bar{x} + \varepsilon_1(\bar{x},\bar{y}) = x', \bar{y} + \varepsilon_2(\bar{x},\bar{y}) = y'$. Then for the new involution $\tilde{h}_2$, we get the following expression

$$\tilde{h}_2 = T^{-1} \circ h_2 \circ T : \begin{cases} \bar{x} + \varepsilon_1(\bar{x},\bar{y}) = -x - \varepsilon_1(x,y) + F(y + \varepsilon_2(x,y)), \\ \bar{y} + \varepsilon_2(\bar{x},\bar{y}) = y + \varepsilon_2(x,y). \end{cases}$$

After this, formula (16) for the map $\hat{H} = h_1 \circ \tilde{h}_2$ is easily obtained: we only need to replace $\bar{x} \leftrightarrow \bar{y}$ in this expression for $\tilde{h}_2$ (x and y are not changed). □

Lemma 3.2. *The Jacobian of the perturbed map $\hat{H}$ is*

$$J(\hat{H}) = \frac{\left(1 + \varepsilon_{2y}(x,y)\right)\left(1 + \varepsilon_{1x}(x,y)\right) - \varepsilon_{2x}(x,y)\varepsilon_{1y}(x,y)}{\left(1 + \varepsilon_{2y}(\bar{y},\bar{x})\right)\left(1 + \varepsilon_{1x}(\bar{y},\bar{x})\right) - \varepsilon_{2x}(\bar{y},\bar{x})\varepsilon_{1y}(\bar{y},\bar{x})} \quad (17)$$

Proof. We calculate the derivatives $\partial\bar{x}/\partial x$, $\partial\bar{y}/\partial x$, $\partial\bar{x}/\partial y$ and $\partial\bar{y}/\partial y$ from (16):

$$\left(1 + \varepsilon_{2y}(\bar{y},\bar{x})\right)\frac{\partial\bar{x}}{\partial x} = \varepsilon_{2x}(x,y) - \varepsilon_{2x}(\bar{y},\bar{x})\frac{\partial\bar{y}}{\partial x},$$

$$\left(1 + \varepsilon_{2y}(\bar{y},\bar{x})\right)\frac{\partial\bar{x}}{\partial y} = 1 + \varepsilon_{2y}(x,y) - \varepsilon_{2x}(\bar{y},\bar{x})\frac{\partial\bar{y}}{\partial y},$$

$$\left(1 + \varepsilon_{1x}(\bar{y},\bar{x})\right)\frac{\partial\bar{y}}{\partial x} = -1 + F'\left(y + \varepsilon_2(x,y)\right)\cdot\varepsilon_{2x}(x,y) - \varepsilon_{1x}(x,y) - \varepsilon_{1y}(\bar{y},\bar{x})\frac{\partial\bar{x}}{\partial x},$$

$$\left(1 + \varepsilon_{1x}(\bar{y},\bar{x})\right)\frac{\partial\bar{y}}{\partial y} = F'\left(y + \varepsilon_2(x,y)\right)\cdot\left(1 + \varepsilon_{2y}(x,y)\right) - \varepsilon_{1y}(x,y) - \varepsilon_{1y}(\bar{y},\bar{x})\frac{\partial\bar{x}}{\partial y}.$$

Solving this system for the partial derivatives, we get the formula (17) for the Jacobian. □

Notice that among the perturbations in the form (16) we can select more simple ones which, nevertheless, preserve reversibility, with respect to the involution h, and destroy conservativity. Let us consider two examples.

Example 1. We consider the case with $\varepsilon_2 \equiv 0$. Then map (16) takes the form

$$\hat{H} :\ \ \bar{x} = y,\ \ \bar{y} = -x + F(y) - \varepsilon_1(x,y) - \varepsilon_1(\bar{y},\bar{x}) \quad (18)$$

and the Jacobian of this map

$$J = \frac{1 + \varepsilon_{1x}(x,y)}{1 + \varepsilon_{1x}(\bar{y},\bar{x})} \quad (19)$$

is not 1 generally. Moreover, if, for example, $\varepsilon_1(x,y) = a_{20}x^2 + a_{11}xy + a_{02}y^2$, then (since $\bar{x} = y$)

$$J = \frac{1 + a_{11}y + 2a_{20}x}{1 + a_{11}\bar{x} + 2a_{20}\bar{y}} = \frac{1 + a_{11}y + 2a_{20}x}{1 + a_{11}y + 2a_{20}\bar{y}},$$

i.e. including quadratic terms xy and x^2 into the perturbation ε_1 makes the Jacobian non-constant.[4]

Other particular case of function $\varepsilon_1(x,y)$ includes, for example, $\varepsilon_1(x,y) = xf_1(y) + f_2(y)$, where $f_1(0) = 0, f_2(0) = f_2'(0) = 0$, i.e. $\varepsilon_1(x,y)$ being linear in x. Then $J = (1 + f_1(y))(1 + f_1(\bar{x}))^{-1} \equiv 1$.

Let us consider another perturbation with $\varepsilon_1(x,y) = p(x) + q(y)$ and $p'(x) = v(x)$. Then $\varepsilon_{1x}(x,y) = v(x)$, $\varepsilon_{1x}(\bar{y},\bar{x}) = v(\bar{y})$ and, by (19),

$$J = \frac{1 + v(x)}{1 + v(\bar{y})}$$

Formally, it means that $J \not\equiv 1$. However, for any periodic orbit, the Jacobian J_n of its first return map will be equal to 1. Indeed, let $M_i(x_i, y_i)$, $i = 1, ..., n$, be the points of an n-periodic orbit P. Then, since $x_i = y_{i-1}$, we obtain that

$$J_n = J(\hat{H}^n)\Big|_{M_1} = \prod_{i=1}^{n} \frac{1 + v(y_{i-1})}{1 + v(y_{i+1})} \equiv 1 \tag{20}$$

since the nominator and denominator of this product contain the same factors. This means that any periodic orbit is conservative, any invariant sets with dense subsets of periodic orbits (for instance, horseshoes) are also conservative etc.

Moreover, we can claim that the dynamics of the map $\hat{H}$ in the form (18) with $\varepsilon_1(x,y) = p(x) + q(y)$ is totally conservative, since this map possesses a smooth invariant measure.

Indeed, as known [31], a measure $d\mu = \rho(x,y)dxdy$ is invariant if and only if the density $\rho(x,y)$ is a fixed point of the Ruelle-Perron-Frobenius operator, i.e.

$$\rho(x,y) = \frac{\rho \circ \hat{H}^{-1}(x,y)}{|J|} = \frac{1 + v(\bar{y})}{1 + v(x)} \cdot \rho \circ \hat{H}^{-1}(x,y).$$

Let us check that the function $\rho(x,y) = (1 + v(y)) \cdot (1 + v(\bar{y}))$ satisfies this relation. For simplicity, take a point (x_0, y_0) and denote its image by $(x_1, y_1) = \tilde{H}(x_0, y_0)$ and the preimage by $(x_{-1}, y_{-1}) = \tilde{H}^{-1}(x_0, y_0)$. Then we have

$$\rho(x_0, y_0) = (1 + v(y_0))(1 + v(y_1)), \quad \rho(x_{-1}, y_{-1}) = (1 + v(y_{-1}))(1 + v(y_0)).$$

Since $x_0 = y_{-1}$ we obtain

$$\frac{1 + v(y_1)}{1 + v(x_0)} \cdot \rho(x_{-1}, y_{-1}) = \frac{1 + v(y_1)}{1 + v(x_0)} \cdot (1 + v(x_0))(1 + v(y_0)) = \rho(x_0, y_0).$$

Therefore, the measure

$$\mu(A) = \int_A (1 + v(y)) \cdot (1 + v(\bar{y}))dxdy$$

is invariant for the map $\tilde{H}$.

Example 2. Consider the case with $\varepsilon_1(x,y) \equiv 0$. Then map (16) takes the form

$$\hat{H}^{(2)}: \quad \bar{x} = y + \varepsilon_2(x,y) - \varepsilon_2(\bar{y},\bar{x}), \quad \bar{y} = -x + F(y + \varepsilon_2(x,y)), \tag{21}$$

[4]In particular, we use such perturbations in Section 4.3 in order to show that nonsymmetric orbits can be non-conservative, see formula (32) below for a special reversible perturbation of the conservative Hénon map.

and

$$J(\hat{H}^{(2)}) = \frac{1+\varepsilon_{2y}(x,y)}{1+\varepsilon_{2y}(\bar{y},\bar{x})},$$

i.e., J is not 1 generally. However, not any perturbations ε_2 are suitable. For example, let function $\varepsilon_{2y}(x,y) = v(x,y)$ be symmetric, i.e. $v(x,y) = v(y,x)$ (as for $\varepsilon_2 = xy^2$). In this case, $J(\hat{H}^{(2)}|_{(x_i,y_i)}) = (1+v(x_i,y_i))(1+v(x_{i+1},y_{i+1}))^{-1}$, and when calculating the Jacobian of a periodic orbit as in (20) we get $J_n = 1$. At the same time, the perturbation $\varepsilon_2 = \alpha xy$ is quite suitable. Indeed, the Jacobian $J = (1+\alpha x)(1+\alpha\bar{y})^{-1}$ is not constant and, moreover, since the function $\varepsilon_2(x,y)$ is linear in y, map (21) can be represented in the explicit form. Note that such perturbations were considered in [11] while studying effects of reversible perturbations on the 1:3 resonance in the conservative cubic Hénon maps.

3.1. **Perturbations of nonorientable conservative Hénon-like maps.** In this section we show that nonorientable conservative Hénon-like maps also admit reversible perturbations of the same types that have been considered in the previous sections for orientable maps.

We consider the nonorientable conservative Hénon-like map of the form

$$H_{-1}: \quad \bar{x} = -y, \quad \bar{y} = -x + F(y). \tag{22}$$

It is easily to show that this map is reversible with respect to the involution $h : (x,y) \to (y,x)$, if function $F(y)$ is even, i.e. $F(-y) = F(y)$ (in particular, it follows from Lemma 3.3 below). By analogy with Lemma 3.1, we consider the following perturbation

$$\hat{H}_{-1}: \quad \bar{x} = -y, \quad \bar{y} = -x + F(y) - \varepsilon(x,y) - \varepsilon(\bar{y},\bar{x}), \tag{23}$$

where $\varepsilon(x,y)$ is some smooth function.

Lemma 3.3. *If $F(y)$ is an even function, $F(y) = F(-y)$, then map $\hat{H}_{-1}$ (given in (23)) is reversible with respect to the involution $h : (x,y) \to (y,x)$, and*

$$J(\hat{H}_{-1}) = -\frac{1+\varepsilon_x(x,y)}{1+\varepsilon_x(\bar{y},\bar{x})}. \tag{24}$$

Proof. The inverse map $(\hat{H}_{-1})^{-1}$ takes the form

$$(\hat{H}_{-1})^{-1}: \quad \bar{x} = -y + F(-x) - \varepsilon(\bar{x},\bar{y}) - \varepsilon(y,x), \quad \bar{y} = -x. \tag{25}$$

After the interchange $x \leftrightarrow y, \bar{x} \leftrightarrow \bar{y}$ in (25) we obtain the map $h \circ \hat{H}_{-1} \circ h$ that coincides with map (23) if $F(-y) = F(y)$, i.e., when $F(y)$ is an even function.

For map $\hat{H}_{-1}$ in the form (23), we have that $J(\hat{H}_{-1}) = -\partial\bar{x}/\partial y \cdot \partial\bar{y}/\partial x$, since $\partial\bar{x}/\partial x \equiv 0$. Then we have

$$\frac{\partial\bar{x}}{\partial y} = -1, \quad \frac{\partial\bar{y}}{\partial x} = -1 - \varepsilon_x(x,y) - \varepsilon_x(\bar{y},\bar{x})\frac{\partial\bar{y}}{\partial x}.$$

This gives us the desired formula (24). □

4. **Symmetry breaking bifurcations in reversible perturbations of Hénon-like maps.** In this section we consider several examples of two-dimensional reversible maps that are perturbations of Hénon-like maps and demonstrate reversible symmetry breaking bifurcations [22] of fixed points or periodic orbits. Even with arbitrarily small perturbations, such bifurcations lead to the appearance of dissipative elements of dynamics, although these bifurcations closely follow the corresponding bifurcations in the unperturbed area-preserving maps. For example, a symmetric couple of elliptic or saddle orbits for an area-preserving map is transformed into a symmetric couple containing sink and source or saddles with the Jacobians greater and less than 1 in the perturbed map, etc. The knowledge of these bifurcations and conditions of their realization is very relevant to understand such phenomenon as the appearance of mixed dynamics at (reversible) perturbations of conservative systems [10, 12, 35].

4.1. **Symmetry breaking bifurcations in the product of two quadratic Hénon maps.** Note that the product of two non-conservative asymmetric Hénon maps H_1 and H_2 of the form (11) with $F(y) = M - y^2$ appears naturally as the normal forms of first return maps near symmetric quadratic homoclinic or heteroclinic tangencies to symmetric periodic orbits of reversible diffeomorphisms [4, 5]. Accordingly, their local bifurcations under reversible perturbations can play a role of global symmetry breaking bifurcations leading to the onset of reversible mixed dynamics.

In this section we consider bifurcations of this type. They are bifurcations of fixed points in some one-parameter family of reversible maps that unfolds the product of two non-conservative Hénon maps

$$H_1 : \bar{x} = y, \bar{y} = M - bx - y^2 \ \text{ and } \ H_2 : \bar{x} = y, b\bar{y} = M - x - y^2$$

with the Jacobians equal to b and b^{-1}, respectively. Their compositions $H_2 \circ H_1$ and $H_1^{-1} \circ H_2^{-1}$ are both area-preserving maps, and, moreover, the latter map $T_2 = H_1^{-1} \circ H_2^{-1}$ can be written in the following cross-form (compare with (12))

$$T_2 : \quad \bar{x} = \frac{1}{b}x - \frac{M}{b} + \frac{1}{b}\bar{y}^2, \ \ y = \frac{1}{b}\bar{y} - \frac{M}{b} + \frac{1}{b}x^2.$$

To study symmetry breaking bifurcations appearing at reversible perturbations of this map we embed it in the following one-parameter family

$$T_{2\mu} : \quad \bar{x} = -\frac{M}{b} + \frac{1}{b}x + \frac{1}{b}\bar{y}^2 + \mu x\bar{y}, \quad y = -\frac{M}{b} + \frac{1}{b}\bar{y} + \frac{1}{b}x^2 + \mu\bar{x}y, \tag{26}$$

where μ is a (small) parameter. This family is a representative of the class (13) of reversible perturbations given by Lemma 2.5, and, thus, it preserves the reversibility with respect to the involution $h : (x, y) \to (y, x)$.

In Figure 1 the main elements of bifurcation diagrams for fixed points of maps T_2 and $T_{2\mu}$ are represented in the (b, M)-parameter plane: in Figure 1(a) for $\mu = 0$ and in Figure 1(b) for a sufficiently small fixed μ. We exclude a small strip containing the axis $b = 0$ from the consideration since maps T_2 and $T_{2\mu}$ are not defined for $b = 0$. The main bifurcation curves are the following: the fold bifurcation curves F_1 and F_2, the reversible pitchfork bifurcation curves PF_1 and PF_2 as well as several period-doubling curves PD that are shown as gray dashed lines in Figure 1. The

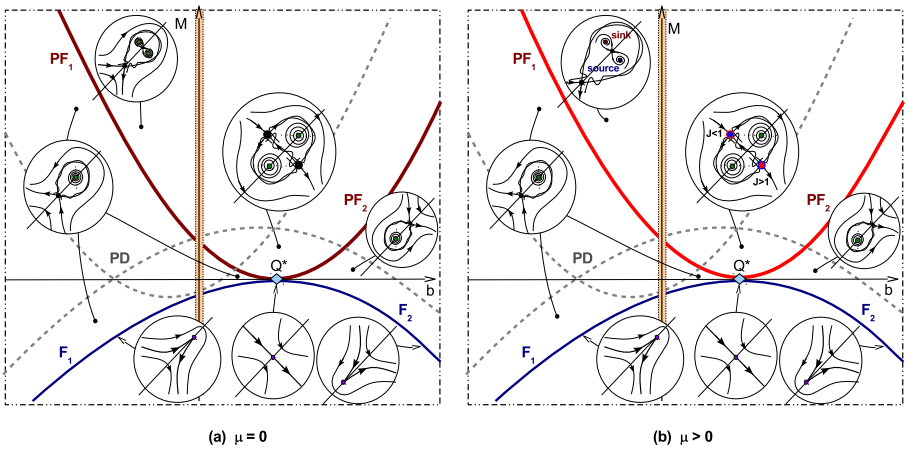

FIGURE 1. Elements of the bifurcation diagram in the (b, M)-parameter plane for the maps (a) T_2 and (b) $T_{2\mu}$ with small fixed μ.

equations of the curves are as follows:

$$\begin{aligned} F_1: &\quad 4(1+b\mu)M = -(b-1)^2, \text{ where } b<0,\\ F_2: &\quad 4(1+b\mu)M = -(b-1)^2, \text{ where } b>0,\\ PF_1: &\quad 4M = (3+b\mu)(b-1)^2, \text{ where } b<0\\ PF_2: &\quad 4M = (3+b\mu)(b-1)^2, \text{ where } b>0. \end{aligned}$$

Curves F_1 and F_2 correspond to a creation of fixed points of T_2 and $T_{2\mu}$. There appears a symmetric parabolic fixed point which is nondegenerate for all values of (b, M) in F_1 and F_2, except for the point $Q^*(b=1, M=0) \in F_2$. The parabolic point bifurcates into 2 symmetric elliptic and saddle fixed points. The transition through point $Q^*(b=1, M=0)$ corresponds to a codimension 2 bifurcation which consists in the emergence of 4 fixed points: 2 symmetric elliptic and 2 saddle fixed points which compose a symmetric couple of points.

In the perturbed case $\mu \neq 0$, the character of the fold and period-doubling bifurcations is not changed qualitatively if μ is sufficiently small. However, the pitchfork bifurcations can give rise to non-conservative fixed points. It follows from Lemma 2.5 that the Jacobian of (26) is

$$J = \frac{1+b\mu\bar{y}}{1+b\mu x} \tag{27}$$

In order to find the fixed points of (26), we equate $\bar{x} = x, \bar{y} = y$ and obtain the following system

$$x(b-1) = y^2 - M + b\mu xy, \quad y(b-1) = x^2 - M + b\mu xy. \tag{28}$$

Subtracting and adding up the equations and taking into account that $x \neq y$ (for asymmetric fixed points) gives us

$$x + y = 1 - b, \quad xy = \frac{(1-b)^2 - M}{1-b\mu}.$$

Thus, if

$$D = \frac{4M - (1-b)^2(3+b\mu)}{4(1-b\mu)} > 0,$$

then two asymmetric fixed points M_1 and M_2 appear for $T_{2\mu}$:

$$M_1 = \left(\frac{1-b}{2} + \sqrt{D}, \frac{1-b}{2} - \sqrt{D}\right) \text{ and } M_2 = \left(\frac{1-b}{2} - \sqrt{D}, \frac{1-b}{2} + \sqrt{D}\right).$$

These two points are symmetric with respect to the line $y = x$ and they merge with the corresponding symmetric fixed point under a reversible pitchfork bifurcation (which occurs when $D = 0$).

It follows from (27) that the Jacobian at fixed points M_1 and M_2 is

$$J_1 = 1 - \frac{4b\mu\sqrt{D}}{2 + b\mu(1-b+2\sqrt{D})}, \quad J_2 = 1 + \frac{4b\mu\sqrt{D}}{2 + b\mu(1-b-2\sqrt{D})},$$

respectively. Thus, if $b\mu > 0$, then $J_1 < 1$ and $J_2 = J_1^{-1} > 1$.

The topological type of these points (for small μ) is easily determined from the conservative approximation $\mu = 0$, see Figure 1a. In the case $b < 0$, points M_1 and M_2 compose a symmetric couple of elliptic fixed points for $\mu = 0$. For $\mu \neq 0$, they are transformed into a symmetric couple of "sink-source" fixed points: points M_1 and M_2 become stable and unstable foci, respectively, if $\mu > 0$. In the case $b > 0$, points M_1 and M_2 become non-conservative saddles for $\mu \neq 0$: with the Jacobians $J_1 < 1$ and $J_2 > 1$, respectively, if $\mu > 0$.

We also note that in the case $|b| = 1$ map $T_{2\mu}$ of the form (26) gives an example of a reversible perturbation for the second iteration of the conservative Hénon map, the orientable one at $b = -1$ and nonorientable at $b = +1$. However, these perturbations are not suitable for the Hénon maps themselves. Thus, at $b = -1$, the curve PF_1 is, in fact, the period-doubling curve for a symmetric fixed point which means that proper reversible perturbations can not lead to symmetry breaking. In the next sections, we consider questions on correct reversible perturbations for the Hénon maps, nonorientable and orientable, and on the structure of the accompanying symmetry breaking bifurcations.

4.2. **Symmetry breaking bifurcations in the nonorientable reversible Hénon maps.** In this section we consider now the nonorientable Hénon map H_{-1} of the form

$$\bar{x} = -y, \bar{y} = -M - x + y^2, \tag{29}$$

that is a particular case of map (22).

For $M < 0$, map (29) has no fixed points or periodic orbits. However, they appear immediately for $M > 0$ under the so-called fold-flip bifurcation occurring at $M = 0$ when the map has a fixed point $P(0,0)$ with eigenvalues $+1$ and -1. For $M > 0$, this point splits into 4 points, see Figure 2, two of them are fixed points S_1 and S_2, and the other two points form a 2-periodic orbit (Q_1, Q_2), i.e. $H_{-1}(Q_1) = Q_2, H_{-1}(Q_2) = Q_1$. Note that points Q_1 and Q_2 are elliptic 2-periodic orbits, and they are also symmetric since they both belong to the symmetry line $x = y$. In contrast, points S_1 and S_2 are saddles and they compose a symmetric couple of points, i.e. $h(S_1) = S_2$ and $h(S_2) = S_1$. The coordinates of these points are

$$Q_1 = (-\sqrt{M}, -\sqrt{M}),\ Q_2 = (\sqrt{M}, \sqrt{M}),\ S_1 = (-\sqrt{M}, \sqrt{M}),\ S_2 = (\sqrt{M}, -\sqrt{M}).$$

All these points are conservative points of map (29).

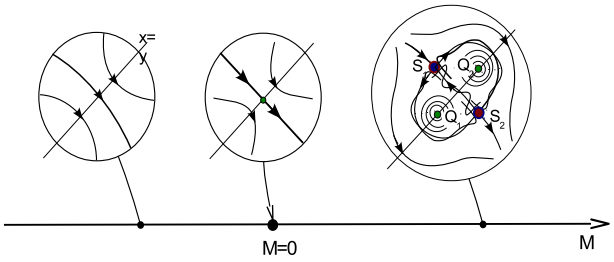

FIGURE 2. Main bifurcations in maps (29) and (30) when μ is small and fixed and M changes. The points Q_1 and Q_2 are symmetric elliptic 2-periodic orbits, while the points S_1 and S_2 are nonorientable saddle fixed points that compose a symmetric couple of points. The points S_1 and S_2 are conservative with the Jacobian -1 for $\mu = 0$ and non-conservative with the Jacobians $-1 < J_1 < 0$ and $J_2 < -1$, respectively, for $\mu > 0$.

However, due to Lemma 3.3, adding reversible perturbations we can destroy the conservativity of fixed points S_1 and S_2. For example, let us consider the following perturbed map

$$\tilde{H}_{-1\mu}: \quad \bar{x} = -y, \quad \bar{y} + \mu\bar{x}\bar{y} = -M - x + y^2 - \mu xy, \tag{30}$$

where we have chosen the perturbation $\varepsilon(x, y) = \mu xy$, being μ a small parameter. By Lemma 3.3, this map is reversible with respect to the involution $h : (x, y) \to (y, x)$, however, it is no longer conservative for $\mu \neq 0$. Indeed, formula (24) for the Jacobian reads as

$$J = -\frac{1+\mu y}{1+\mu\bar{x}} = -\frac{1+\mu y}{1-\mu y}.$$

Fixed points of map (30) are easily found: $S_1 = (-a(\mu), a(\mu))$, $S_2 = (a(\mu), -a(\mu))$, where $a(\mu) = \sqrt{M/(1+2\mu)}$. Then we have that the Jacobians J_1 and J_2 at points S_1 and S_2 are

$$J_1 = -1 - \frac{2\mu\sqrt{M}}{\sqrt{1+2\mu} - \mu\sqrt{M}}, \quad J_2 = -1 + \frac{2\mu\sqrt{M}}{\sqrt{1+2\mu} + \mu\sqrt{M}},$$

respectively. Thus, if $M > 0$ and $\mu > 0$ is not very large, the points S_1 and S_2 compose a symmetric couple of (nonorientable) saddles with the Jacobians $J_1 < -1$ and $-1 < J_2 = J_1^{-1} < 0$.

4.3. **Symmetry breaking bifurcations in the orientable reversible Hénon maps.** In this section we consider the standard area-preserving and orientable Hénon map H_{1+} of the form

$$\bar{x} = y, \quad \bar{y} = M - x - y^2, \quad . \tag{31}$$

Bifurcations of its fixed points are well-known and include a parabolic bifurcation at $M = -1$, giving rise to symmetric elliptic and saddle fixed points, and a conservative period-doubling bifurcation of the fixed elliptic point at $M = 3$, after which the elliptic fixed point becomes saddle and an elliptic 2-periodic orbits are

born. Besides, when M changes from $M = -1$ to $M = 3$, the symmetric elliptic fixed point undergoes infinitely many bifurcations related to the appearance of resonant periodic orbits of period q in its neighbourhood – whenever the eigenvalues $e^{\pm i\varphi}$ pass through the values $\varphi = 2\pi\frac{p}{q}$, where p and q are mutually prime natural numbers and $p < q$.

However, as it is well-known, the fixed points and 2-periodic orbits in the Hénon map are symmetric. The resonant periodic points are also symmetric if the resonances are nondegenerate. Thus, 3-periodic and 5-periodic resonant orbits are symmetric. Although, the 1:4 resonance (related to eigenvalues $e^{\pm i\pi/2} = \pm i$) is degenerate in the Hénon map [2, 33] (the so-called Arnold degeneracy [1] takes place here), this bifurcation is not of symmetry breaking type.

A simple calculation of the number of points in periodic orbits of periods $n = 1$, 2, 3 and 4 (this number cannot be greater than 2^n, by Bezout's theorem, even if we include all points of periodic orbits of periods divisors of n)

- period 1 (fixed points) – two points;
- period 2 – two points (not including 2 fixed points) that compose one 2-periodic orbit appearing after the period-doubling bifurcation of the elliptic fixed point;
- period 3 – 6 points (we exclude 2 fixed points and the remaining 6 points compose two (elliptic and saddle) 3-periodic orbits accompanying the 1:3 resonance);
- period 4 – 12 points (we exclude 2 fixed points and 2 points of the 2-periodic orbits and, thus, the remaining 12 points form two 4-periodic orbits born from the 1:4 resonance and one 4-periodic orbit appearing after a period-doubling bifurcation of the elliptic 2-periodic orbit);

shows that there are no asymmetric periodic orbits of these periods.

The case of period 5 points is more delicate. If two fixed points are excluded, then 30 more points remain. 20 such points compose four 5-periodic orbits born from the 1:5 and 2:5 resonances. Concerning remaining 10 points, they appear at a symmetric parabolic bifurcation of a 5-periodic orbit. The last bifurcation we have found numerically at $M = 5.5517$. The y-coordinates of the corresponding symmetric parabolic point is $y_1 = y_2 = -2.243751084, y_3 = y_5 = 2.761032157, y_4 = 0.172152512$.

The calculation of the number of points of 6-periodic orbits shows the following. There are 64 such points in total. They include 10 points of smaller periods: 2 fixed points, 2 points of the 2-periodic orbit and 6 points of the 3-periodic orbits. The remaining 54 points form 9 orbits of period 6. Among them, 5 orbits are symmetric – two 6-periodic orbits are born from the 1:6 resonance, one periodic orbit appears via a period-doubling bifurcation of the elliptic 3-periodic orbit, and two orbits arise due to the 1:3 resonance of a 2-periodic elliptic orbit.

The remaining 4 orbits of period 6 may be asymmetric. For example, some of these orbits can appear as a result of a symmetry breaking bifurcation when a symmetric couple of two parabolic 6-periodic orbits appears and then splits into two symmetric couples of elliptic and saddle 6-periodic orbits. Other possible cases can be related to two bifurcations of symmetric 6-periodic orbits and at least one of these bifurcations is a pitchfork bifurcation. We show below, see Section 4.4, that the second possibility is indeed realized in the Hénon map H_{+1}.

We have found numerically a couple of such orbits O_6^1 and O_6^2 (appearing after the pitchfork bifurcation). In particular, for $M = 4$, the orbit $O_6^1 = \{(x_i, y_i)\}$,

$i = 1, ..., 6$, where $x_{i+1} = y_i$, has the following y-coordinates

$$y_1 = -1.860805853, y_2 = 2.472833909, y_3 = -0.254101688,$$
$$y_4 = 1.462598423, y_5 = 2.114907541, y_6 = -1.935432332.$$

The orbit $O_6^2 = \{(\tilde{x}_i, \tilde{y}_i)\}$, $i = 1, ..., 6$ is symmetric to O_6^1 and, thus, has coordinates $\tilde{x}_i = y_i$ and $\tilde{y}_i = \tilde{x}_i = y_{i-1}$.

Now we consider the reversible perturbation of Hénon map H_{+1} as follows

$$\tilde{H}_{+1\mu}: \quad \bar{x} = y, \bar{y} + \mu(\bar{x}\bar{y} + \bar{y}^2) = M - x - y^2 - \mu(xy + x^2), \tag{32}$$

that preserve reversibility with respect to the involution $h : (x, y) \to (y, x)$ due to Lemma 3.1, see also Example 1 in Section 3 for $\varepsilon_1(x, y) = \mu(xy + y^2)$.

We find that, in the perturbed map (32), the orbit O_6^1 has at $M = 4$, $\mu = 0.01$ the following y_i-coordinates (here again $x_{i+1} = y_i$)

$$y_1 = -1.833980679, y_2 = 2.460965013, y_3 = -0.2062196180,$$
$$y_4 = 1.423687035, y_5 = 2.107429699, y_6 = -1.911473368.$$

We calculate the Jacobian of map (32) at O_6^1

$$J_1 = \prod_{i=1}^{6} \frac{1 + \mu y_i + 2\mu y_{i-1}}{1 + \mu y_i + 2\mu y_{i+1}}$$

and obtain that $J_1 = 0.9999999555$. By the symmetry, the orbit O_6^2 has the Jacobian $J_2 = J_1^{-1}$.

4.4. **Search of the asymmetric 6-periodic orbit in H_{1+}.** It is quite surprising that symmetry breaking bifurcations in the conservative Hénon map H_{1+}, given in (31), begin only from 6-periodic orbits and, moreover, it is even more surprising that such bifurcations can be studied analytically.[5]

The corresponding bifurcation scenario, including a pitchfork bifurcation of a 6-periodic orbit, starts at the value $M = M_1 = \frac{5}{4}$ when an elliptic 3-periodic orbit O_3 undergoes a supercritical period-doubling bifurcation after which the orbit O_3 becomes a symmetric saddle 3-periodic orbit and a symmetric elliptic 6-periodic orbit O_6 is born in its neighbourhood, see Figures 3 and 4 (a) and (b). When increasing M, two successive period-doubling bifurcations with the orbit O_6, supercritical (at $M = M_2 \approx 1.2813$) and subcritical (at $M = M_3 \approx 2.98038$), take place. For $M_2 < M < M_3$ the orbit $\tilde{O}_6$ is saddle, and for $M > M_3$ it becomes elliptic again. The mentioned above pitchfork bifurcation occurs at $M = M_4 = 3$ when the orbit O_6 becomes a symmetric saddle 6-periodic orbit and a symmetric couple of elliptic 6-periodic orbits O_6^1 and O_6^2 is born, see Figures 3 and 4 (c) and (d).[6]

Consider now the orbit O_6 and its bifurcations in more detail. We use the fact that this orbit is symmetric and has two intersection points with the line $x = y$.

[5] We are not aware of the corresponding results, although it is possible that they exist somewhere, since the Hénon map and its bifurcations are one of the most popular topics in the theory of dynamical systems. In this regard, we consider to be rather necessary and in any case useful to include in this article some results of the analytical study of symmetry breaking bifurcations in the conservative Hénon map.

[6] Note that the orbit O_3 appears in H_{1+} at $M = 1$ as a result of a parabolic bifurcation leading to the birth of symmetric 3-periodic elliptic and saddle orbits O_3 and S_3. When further increasing M, the orbits O_3 and S_3 undergo first bifurcations simultaneously, at $M = 5/4$. But these bifurcations are completely different: for O_3, this is the above period-doubling bifurcation; for S_3, this is a bifurcation of creation of the 1:3 resonance, when 3 points of S_3 collapse into one point, the fixed point $O_{1:3}(\frac{1}{2}, \frac{1}{2})$ with eigenvalues $e^{\pm 2\pi/3}$ (the 1:3 resonance).

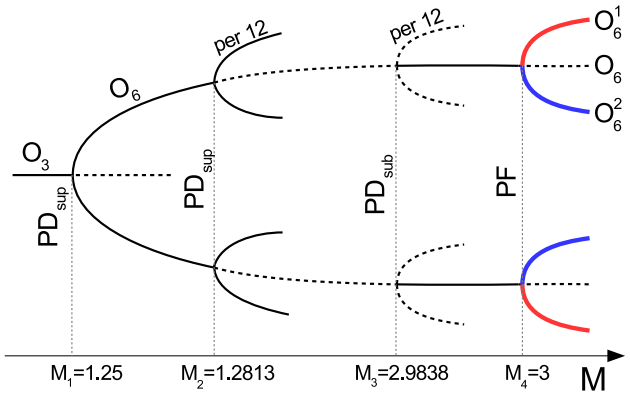

FIGURE 3. A schematic tree for the bifurcation scenario of the appearance of a symmetric couple of 6-periodic orbits in the third power of Hénon map H_{1+}.

Let $\{p_i(x_i, y_i)\}$, $i = 1, 2, ..., 6$, be successive points of O_6, i.e., $p_{i+1} = H_{1+}(p_i)$ and $p_1 = H_{1+}(p_6)$. Then the coordinates (x_i, y_i) satisfy the following equations

$$x_{i+1} = y_i,\ y_{i+1} = M - x_i - y_i^2,\ i = 1, ..., 5,\ x_1 = y_6,\ y_1 = M - x_6 - y_6^2.$$

Since $x_{i+1} = y_i$, we can reduce this system to the following system of 6 quadratic equations

$$\begin{array}{c} y_2 = M - y_6 - y_1^2,\ y_3 = M - y_1 - y_2^2,\ y_4 = M - y_2 - y_3^2, \\ y_5 = M - y_3 - y_4^2,\ y_6 = M - y_4 - y_5^2,\ y_1 = M - y_5 - y_6^2. \end{array} \tag{33}$$

Assume that the point $p_1(x_1, y_1)$ of O_6 belongs to the symmetry line $x = y$, i.e. $x_1 = y_1$. Then the point $p_4 = H_{1+}^3(P_1)$ is also symmetric, i.e. $x_4 = y_4$. Since $x_1 = y_6$ and $x_4 = y_3$, it follows that $y_6 = y_1$ and $y_3 = y_4$. Then we get from the first and the last equations of (33) that $y_2 = y_5$ and, thus, the system (33) is reduced to the following system of three equations

$$y_1 + y_2 = M - y_1^2,\ y_1 + y_3 = M - y_2^2,\ y_2 + y_3 = M - y_3^2, \tag{34}$$

From the first and last equations of (34) we obtain the relation $y_1 - y_3 = (y_3 - y_1)(y_3 + y_1)$. Since $y_1 \neq y_3$ (when $y_1 = y_3$ the corresponding orbit has period 3), it follows that $y_1 + y_3 = -1$. Then the second equation of (34) gives us that $y_2^2 = M + 1$. Thus, y_1 and y_3 satisfy the following relations

$$y_1^2 + y_1 - M \pm \sqrt{M+1} = 0,\ y_3^2 + y_3 - M \pm \sqrt{M+1} = 0.$$

Among various solutions of this system of quadratic equations, only the solution

$$y_1 = \frac{1}{2}\left(-1 - \sqrt{1 - 4\sqrt{M+1} + 4M}\right), y_3 = \frac{1}{2}\left(-1 + \sqrt{1 - 4\sqrt{M+1} + 4M}\right)$$

(or that the one when y_1 and y_3 are swapped) is suitable for O_6. Indeed, both these solutions exist at $M \geq \frac{5}{4}$ and $y_1 \neq y_3$ if $M > \frac{5}{4}$. Thus, we have found the following y_i-coordinates of points p_i of the orbit O_6:

$$y_1 = y_6 = \frac{1}{2}\left(-1 - \sqrt{1 - 4\sqrt{M+1} + 4M}\right), y_2 = y_5 = \sqrt{M+1},$$

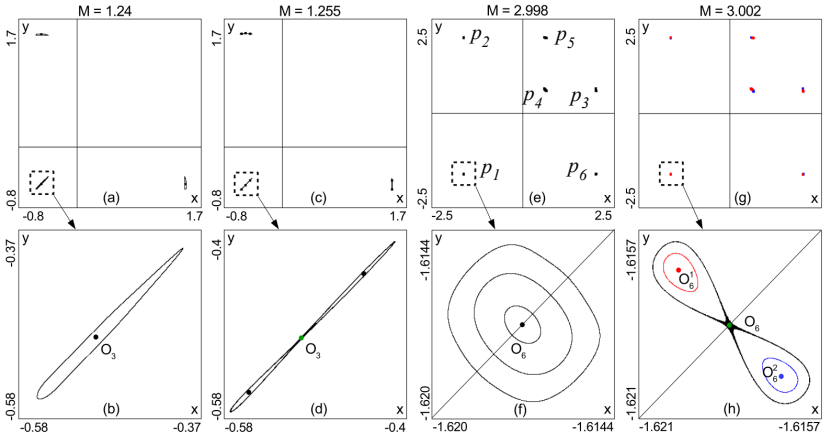

FIGURE 4. Phase portraits of 3- and 6-periodic orbits for the Hénon map H_{+1}: the bottom plots are magnifications of some important details of the top plots.

$$y_3 = y_4 = \frac{1}{2}\left(-1 + \sqrt{1 - 4\sqrt{M+1} + 4M}\right).$$

For analysis of bifurcations of the orbit O_6, we calculate, first, the trace Tr of the characteristic matrix for the map H_{1+}^6 at some point of O_6. As result, we obtain that

$$Tr = 86 + 24\sqrt{M+1} + 116M - 128\sqrt{M+1}M + 96M^2 - 128\sqrt{M+1}M^2 + 64M^3.$$

If we denote $\sqrt{M+1} = x$ $(x > 0)$, we obtain the polynomial

$$Tr(x) = 2+24x+116x^2+128x^3-96x^4-128x^5+64x^6 = 2+4x(2x+1)^3(2x-3)(x-2)$$

Thus, the equation $Tr(x) = 2$ has the solutions $x = 0$, $x = -\frac{1}{2}$ (the triple root) and two positive solutions $x = \frac{3}{2}$ and $x = 2$. The root $x = \frac{3}{2}$ corresponds to the value $M = \frac{5}{4}$ when the orbit O_6 is born. The root $x = 2$ corresponds to the value $M = 3$ when the symmetric elliptic orbit O_6 undergoes a pitchfork bifurcation – the elliptic orbit becomes symmetric saddle and a symmetric couple of elliptic 6-periodic orbits O_6^1 and O_6^2 emerges, see Figures 4(e)-(h). Namely, the orbits O_6^1 and O_6^2 are considered in Section 4.3.

Acknowledgments. The authors thank D.V. Turaev and A.O. Kazakov for very useful remarks. This work is partially supported by the Russian Science Foundation under grants 19-11-00280 (Sections 1, 2 and 3) and 19-71-10048 (Sections 4.3 and 4.4), as well as the Russian Foundation for Basic Research under grants 19-01-00607 (Sections 4.1 and 4.2). S.Gonchenko and K.Safonov thank the Ministry of Science and Higher Education of the Russian Federation, projects No. 075-15-2019-1931 (numerical experiments in Section 4) for support of scientific researches. M. Gonchenko was partially supported by the Spanish grants Juan de la Cierva-Incorporacion IJCI-2016-29071, PGC2018-098676-B-I00 (AEI/FEDER/UE) and the Catalan grant 2017SGR1374.

REFERENCES

[1] V. I. Arnold, *Geometrical Methods in the Theory of Ordinary Differential Equations*, $2^n d$ edition, Springer-Verlag, NY, 1996.

[2] V. S. Biragov, Bifurcations in a two-parameter family of conservative mappings that are close to the Hénon mapping, *Selecta Math. Soviet*, **9** (1990), 273–282.

[3] R. L. Devaney, Reversible diffeomorphisms and flows, *Trans. Am. Math. Soc.*, **218** (1976), 89–113.

[4] A. Delshams, S. V. Gonchenko, V. S. Gonchenko, J. T. Lazaro and O. Sten'kin, Abundance of attracting, repelling and elliptic orbits in two-dimensional reversible maps, *Nonlinearity*, **26** (2013), 1–33.

[5] A. Delshams, M. Gonchenko, S. V. Gonchenko, and J. T. Lazaro, Mixed dynamics of 2-dimensional reversible maps with a symmetric couple of quadratic homoclinic tangencies, *Discrete Contin. Dyn. Syst.*, **38** (2018), 4483–4507.

[6] A. A. Emelianova, V. I. Nekorkin, On the intersection of a chaotic attractor and a chaotic repeller in the system of two adaptively coupled phase oscillators, *Chaos*, **29** (2019), 111102.

[7] A. A. Emelianova, V. I. Nekorkin, The third type of chaos in a system of two adaptively coupled phase oscillators, *Chaos*, **30** (2020), 051105.

[8] A. S. Gonchenko, S. V. Gonchenko, A. O. Kazakov and D. V. Turaev, On the phenomenon of mixed dynamics in Pikovsky-Topaj system of coupled rotators, *Phys. D*, **350** (2017), 45–57.

[9] M. Gonchenko, S. Gonchenko and I. Ovsyannikov, Bifurcations of cubic homoclinic tangencies in two-dimensional symplectic maps, *Math. Model. Nat. Phenom.*, **12** (2017), 41–61.

[10] S. Gonchenko, Reversible mixed dynamics: A concept and examples, *Discontinuity, Nonlinearity, and Complexity*, **5** (2016), 345–354.

[11] M. S. Gonchenko, A. O. Kazakov, E. A. Samylina and A. I. Shyhmamedov, On the 1:3 resonance under reversible perturbations of conservative cubic Hénon maps, preprint, 2020.

[12] S. V. Gonchenko and D. V. Turaev, On three types of dynamics and the notion of attractor, *Proc. Steklov Inst. Math.*, **297** (2017), 116–137.

[13] S. V. Gonchenko, A. S. Gonchenko and A. O. Kazakov, Richness of chaotic dynamics in nonholonomic models of a Celtic stone, *Regu. Chaotic Dyn.*, **18** (2013), 521–538.

[14] S. V. Gonchenko, D. V. Turaev and L. P. Shilnikov, On the existence of Newhouse domains in a neighborhood of systems with a structurally unstable Poincare homoclinic curve (the higher-dimensional case), *Dokl. Math.*, **47**(1993), 268–273.

[15] S. V. Gonchenko, D. V. Turaev and L. P. Shil'nikov, On Newhouse domains of two-dimensional diffeomorphisms that are close to a diffeomorphism with a structurally unstable heteroclinic contour, *Proc. Steklov Inst. Math.*, **216** (1997), 70–118.

[16] S. V. Gonchenko, J. S. V. Lèmb, I. Rios and D. Turaev, Attractors and repellers in the neighborhood of elliptic points of reversible systems, *Dokl. Math.*, **89** (2014), 65–67.

[17] S. V. Gonchenko, M. S. Gonchenko and I. O. Sinitsky, On mixed dynamics of two-dimensional reversible diffeomorphisms with symmetric non-transversal heteroclinic cycles, *Izv. Ross. Akad. Nauk Ser. Mat.*, **84** (2020), 27–59.

[18] A. O. Kazakov, On the appearance of mixed dynamics as a result of collision of strange attractors and repellers in reversible systems, *Radiophysics and Quantum Electronics*, **61** (2019), 650–658.

[19] A. O. Kazakov, Merger of a Hénon-like attractor with a Hńon-like repeller in a model of vortex dynamics, *Chaos*, **30** (2020), 011105.

[20] J. S. W. Lamb and J. A. G. Roberts, Time-reversal symmetry in dynamical systems: A survey, *Phys. D*, **112** (1998), 1–39.

[21] J. S. W. Lamb and O. V. Stenkin, Newhouse regions for reversible systems with infinitely many stable, unstable and elliptic periodic orbits, *Nonlinearity*, **17** (2004), 1217–1244.

[22] L. M. Lerman and D. V. Turaev, Breakdown of symmetry in reversible systems, *Reg. Chaotic Dyn.*, **17** (2012), 318–336.

[23] S. E. Newhouse, The abundance of wild hyperbolic sets and nonsmooth stable sets for diffeomorphisms, *Inst. Hautes Études Sci. Publ. Math.*, **50** (1979), 101–151.

[24] S. E. Newhouse, Diffeomorphisms with infinitely many sinks, *Topology*, **13** (1974), 9–18.

[25] J. Palis and M. Viana, High dimension diffeomorphisms displaying infinitely many periodic attractors, *Ann. of Math. 2*, **140** (1994), 207–250.

[26] A. Politi, G. L. Oppo and R. Badii, Coexistence of conservative and dissipative behaviour in reversible dynamicla systems, *Phys. Rev. A*, **33** (1986), 4055–4060.

[27] T. Post, H. W. Capel, G. R. W. Quispel and J. R. van der Weele, Bifurcations in two-dimensional reversible maps, *Phys. A*, **164** (1990), 625–662.
[28] J. A. G. Roberts and G. R. W. Quispel, Chaos and time-reversal symmetry. Order and chaos in reversible dynamical systems, *Phys. Rep.*, **216** (1992), 63–177.
[29] N. Romero, Persistence of homoclinic tangencies in higher dimensions, *Ergodic Theory Dynam. Systems.*, **15** (1995), 735–757.
[30] D. Ruelle, Small random perturbations of dynamical systems and the definition of attractors, *Comm. Math. Phys.*, **82** (1981), 137–151.
[31] D. Ruelle, *Thermodynamic Formalism: The Mathematical Structures of Classical Equilibrium Statistical Mechanics*, Addison-Wesley Publishing Co., Reading, MA, 1978.
[32] M. B. Sevryuk, *Reversible Systems*, Lect. Notes Math., Vol. 1211, Springer-Verlag, Berlin, 1986.
[33] C. Simó and A. Vieiro, Resonant zones, inner and outer splitting in generic and low order resonances of area preserving maps, *Nonlinearity*, **22** (2009), 1191–1245.
[34] D. Turaev, Richness of chaos in the absolute Newhouse domain, *in Proc. Int. Congr. Math., Hyderabad (India)*, **3** (2010), 1804–1815.
[35] D. Turaev, Maps close to identity and universal maps in the Newhouse domain, *Commun. Math. Phys.*, **335** (2015), 1235–1277.

Received May 2020; 1st revision July 2020; 2nd revision August 2020.

E-mail address: marina.gonchenko@upc.edu
E-mail address: sergey.gonchenko@mail.ru
E-mail address: safonov.klim@yandex.ru